



# Triangular gold nanoparticles conjugated with peptide ligands: A new class of inhibitor for *Candida albicans* secreted aspartyl proteinase



Ali Jebali<sup>a,\*</sup>, Farzaneh Haji Esmaeil Hajjar<sup>b</sup>, Seyedhossein Hekmatimoghaddam<sup>c</sup>, Bahram Kazemi<sup>d,e</sup>, Jesus M. De La Fuente<sup>f,g,h</sup>, Mohsen Rashidi<sup>i</sup>

<sup>a</sup> Department of Genetics, Research and Clinical Center for Infertility, Shahid Sadoughi University of Medical Sciences, Yazd 8916733754, Iran

<sup>b</sup> Department of Microbiology, Pars Hospital Lab, Tehran, Iran

<sup>c</sup> Department of Laboratory Sciences, School of Paramedicine, Shahid Sadoughi University of Medical Sciences, Yazd, Iran

<sup>d</sup> Cellular and Molecular Biology Research Center, Shahid Beheshti University of Medical Sciences, Tehran, Iran

<sup>e</sup> Department of Biotechnology, Shahid Beheshti University of Medical Sciences, Tehran, Iran

<sup>f</sup> Instituto de Nanociencia de Aragón (INA), Universidad de Zaragoza, Mariano Esquillor s/n, 50018 Zaragoza, Spain

<sup>g</sup> Fundacion ARAID

<sup>h</sup> Institute of Nano Biomedicine and Engineering, Key Laboratory for Thin Film and Microfabrication Technology of the Ministry of Education, Research Institute of Translation Medicine, Shanghai Jiao Tong University, Dongchuan Road 800, 200240 Shanghai, People's Republic of China

<sup>i</sup> Department of Pharmacology, School of Medicine, Shahid Beheshti University of Medical Sciences, Tehran, Iran

## ARTICLE INFO

### Article history:

Received 23 March 2014

Accepted 21 May 2014

Available online 2 June 2014

### Keywords:

Triangular gold nanoparticle  
Peptide ligand  
Secreted aspartyl proteinase  
*Candida albicans*

## ABSTRACT

The aim of this study was to find the peptide ligands to inhibit *Candida albicans* secreted aspartyl proteinase 2 (Sap2). First, a ligand library, containing 300 different peptides, was constructed, and their interaction with Sap2 was separately calculated by molecular dynamic software. Second, 10 peptide ligands with the lowest intermolecular energy were selected. Then, triangular gold nanoparticles were synthesized, and separately conjugated with the peptide ligands. After synthesis, antifungal property and Sap inactivation of conjugated triangular gold nanoparticles, peptide ligands, and naked triangular gold nanoparticle were separately assessed, against thirty clinical isolates of *C. albicans*. In this study, we measured the uptake of conjugated and naked nanoparticles by atomic adsorption spectroscopy. This study showed that naked triangular gold nanoparticle and all conjugated triangular gold nanoparticles had high antifungal activity, but no peptide ligands had such activity. Of 300 peptide ligands, the peptide containing N-Cys-Lys-Lys-Arg-Met-Met-Lys-Ser-Met-Cys-C and its conjugate had the highest capability to inhibit Sap. Moreover, the uptake assay demonstrated that triangular gold nanoparticles conjugated with the peptide ligand had the highest uptake.

© 2014 Elsevier Inc. All rights reserved.

## 1. Introduction

Extracellular hydrolytic enzymes (EHs) are important factors for the pathogenic fungi such as *Aspergillus fumigatus* [1], *Trichophyton mentagrophytes* [2], *Cryptococcus neoformans* [3], and *Candida albicans* [4]. There are three important EHs produced by *C. albicans* including secreted aspartyl proteinases (Sap), phospholipase B enzymes, and lipases [4–6]. Based on the previous studies, Sap proteinases which encoded by 10 genes are the key virulence factor of *C. albicans* [7,8]. Of the 10 Sap genes, Sap2 is the major gene which encodes a pre-pro-protein with 342 residues

and molecular mass of 35,880 Da [9]. Moreover, other *Candida* species including *Candida dubliniensis* [10], *Candida tropicalis* [11], and *Candida parapsilosis* express Sap genes [12]. Importantly, Sap enzymes can be inhibited and inactivated by antibody [13]. The protective effect of antibody opens up a new window of research to treat *C. albicans* infections. Another inhibitor of Sap enzymes is pepstatin which can digest mucin and mucosal proteins [14]. Pichova et al. [15] showed that peptidomimetic inhibitors which derived from pepstatin A, could inactivate Sap enzymes extracted from *C. albicans*, *C. tropicalis*, *C. parapsilosis*, and *Candida lusitanae*. Moreover, some renin inhibitors such as A-70450 and A-79912 can also inhibit Sap enzymes. Although both A-70450 and A-79912 are effective to inhibit Sap2 activity in vitro, they are ineffective to decrease the virulence of disseminated candidiasis in the mouse model [16].

Ligand/enzyme interactions, based on three-dimensional structures, have been developed in the recent years. Now, the

\* Corresponding author. Tel.: +98 3518286481; fax: +98 3517256458; mobile: +98 9390348478.

E-mail address: [alijebal2011@gmail.com](mailto:alijebal2011@gmail.com) (A. Jebali).

structural information of enzymes and ligands can be loaded and analyzed in the computer, and the best ligand is introduced [17,18]. Note, ligands which extracted from softwares are not fully trusty, and must be confirmed by the experimental tests. The aim of this study was to find some peptide ligands to inhibit *C. albicans* Sap enzyme. In the next step, all peptide ligands were evaluated by different tests including antifungal assessment, uptake assay, and Sap activity test. On the other hand, we conjugated peptide ligands with triangular gold nanoparticles, and their antifungal property, uptake, and Sap activity were compared with triangular gold nanoparticles and peptide ligands alone.

## 2. Materials and methods

### 2.1. Materials

Hydrogen tetrachloroaurate (HAuCl<sub>4</sub>), triethanolamine (TEA), hexadecyl trimethyl ammonium bromide (CTAB), Sn(IV) meso-tetra(*N*-methyl-4-pyridyl) porphine tetratosylate chloride (SntMepyP), bovine serum albumin (BSA), pepstatin A, and trichloroacetic acid (TCA) were purchased from Sigma–Aldrich chemical company, USA. Sabouraud dextrose agar (SDA), Sabouraud dextrose broth (SDB), RPMI1640, Mueller–Hinton agar medium supplemented with 2% glucose, yeast carbon base (YCB) medium were purchased from Invitrogen, UK. Ammonia, HNO<sub>3</sub>, and sodium citrate buffer were provided from Zyst Fannaver Shargh Company.

### 2.2. Simulation study

In this section, a peptide ligand library, containing 300 different peptides (containing 10 residues), was made. It was based on X-ray crystallography and three-dimensional model of *C. albicans* Sap2 enzyme [17]. The pdb file of Sap enzyme was from protein data bank, DOI:10.2210/pdb1zap/pdb. In the next step, Sap2 and peptide ligands were separately modeled in Ascalaph Designer 1.8.69 software, and simulated for 100 ps in NVT ensemble at 300 K.

In this study, force field and topology parameters were assigned from AMBER 99. Also, TIP3P water model was used to solvate. The energy minimization was carried out in a continuum medium of relative permittivity  $\epsilon = 4r_{ij}$ , and steepest descent were done by conjugate gradient minimization (500 iterations) until the gradient fell below 0.05 kcal/mol/Å. Finally, intermolecular energy was separately measured for each peptide ligand and Sap2 enzyme, and 10 peptides with lowest intermolecular energy were selected.

### 2.3. Synthesis and characterization of triangular gold nanoparticles

First, 10 mL of 20 mM HAuCl<sub>4</sub> was added to 250 mL of 0.2 M TEA/0.1 M ammonia. Next, 250 mL of 10 mM CTAB, 50 mL of 3 mM SntMepyP, and 1000 mL of water were added, and irradiated for 1 h by a discharge lamp (ZFS Company, Iran). To characterize triangular gold nanoparticles, UV-VIS spectrophotometer (Novin gostar Company, Iran), transmission electron microscopy (TEM) (Hitach, Japan), and dynamic light scattering (DLS) (ZFS Company, Iran) were used [19].

### 2.4. Conjugation of selected peptide and triangular gold nanoparticles

One mL of each peptide (64 µg/mL) which synthesized by ZFS Company, was added to 1 mL of synthesized triangular gold nanoparticles (10 µg/mL), incubated for 1 h at 37 °C. After incubation, the tube was centrifuged at 10,000 rpm for 15 min, and unbound peptides were removed. To confirm conjugation, Fourier transform infrared spectroscopy (FTIR) (ZFS Company, Iran) and mass spectroscopy (MS) (ZFS Company, Iran) were used. Finally, the serial concentrations (2, 4, 8, 16, 32, 64 and 128 µg/mL)

of conjugated triangular gold nanoparticles were prepared in the distilled water. Note, the conjugation was done for each peptide ligand. Finally, we had 10 ligand peptides and 10 conjugated triangular gold nanoparticles.

### 2.5. Preparation of *Candida albicans* isolates and culture condition

Thirty clinical isolates of *C. albicans* were obtained from patients suffering from vaginal candidiasis. These patients were from different health center of Yazd and Tehran city, Iran. The isolates were previously confirmed by CHROMagar (BD Diagnostics, USA) and RFLP-PCR at Shahid Beheshti University of Medical Sciences, Tehran, Iran. All isolates were first inoculated on SDA, incubated for 48 h at 37 °C, and then one colony of each isolate was immersed to 10 mL of SDB. After 24 h incubation at 37 °C, *Candida* cells were harvested by centrifugation (1500 rpm, 10 min), washed with phosphate buffered saline, and 10 mL of RPMI1640 medium was added to reach to 10<sup>5</sup> cells/mL.

### 2.6. Minimum inhibitory concentration (MIC)

MIC50 and MIC90 were determined by micro-dilution method [20], according to Clinical and Laboratory Standards Institute, CLSI). First, 100 µL of serial concentrations of conjugated triangular gold nanoparticles, peptide ligands, and triangular gold nanoparticles alone was separately added to 100 µL of each *Candida* suspension. The final concentration of all materials was 1, 2, 4, 8, 16, 32, and 64 µg/mL. After 48 h incubation at 35 °C, their MIC50 and MIC90 were measured, according to control.

### 2.7. Inhibition zone

Agar disk diffusion method was done to find the quantity of inhibition zone [20], according to CLSI. First, 5 µL of each conjugated triangular gold nanoparticle, peptide ligand, and triangular gold nanoparticle at concentration of 64 µg/mL was added on Whatman (Cole-Parmer Co., USA) filter (pore size 20–25 µm, 5 × 5 mm), and dried at 37 °C. Next, 100 µL of *Candida* suspension of each isolate was separately swabbed on Mueller–Hinton agar medium supplemented with 2% glucose in three directions. Then, Whatman papers were placed on them and incubated at 35 °C for 48 h. After incubation, the inhibition zone diameter of each isolate against each material was read.

### 2.8. Uptake assay

First, 100 µL of each conjugated triangular gold nanoparticle, and triangular gold nanoparticle alone at three concentrations (16, 32, and 64 µg/mL) was separately added to 100 µL of each *Candida* suspension (10<sup>5</sup> cells/mL), and incubated for 24 and 48 h at 35 °C. To remove free nanoparticles, *Candida* cells were washed three times with normal saline. Then, 100 µL of 10 M HNO<sub>3</sub> was added to them, and incubated for 24 h at 25 °C. Finally, the quantity of gold atom in each well was quantified by atomic adsorption spectroscopy (AAS) [21,22].

### 2.9. Growth of *Candida albicans* isolates in YCB-BSA medium

Each *C. albicans* isolate was first cultured in YCB-BSA medium, incubated for 24 h at 35 °C. After incubation, the cells were washed with normal saline twice, and then inoculated (10<sup>6</sup> cells) into new YCB-BSA medium [23]. In the next step, 100 µL of conjugated triangular gold nanoparticles, peptide ligands, and triangular gold nanoparticle alone at three concentrations (16, 32, and 64 µg/mL) was added to *Candida* suspension, and incubated for 24 and 48 h at 35 °C.

**Table 1**

The sequence selected peptide ligands and intermolecular energy between each peptide and Sap.

Name	Sequence	Intermolecular energy (kcal/mol)
Peptide ligand 1	N-Cys-Ala-Lys-Ala-Lys-Lys-Ala-Ala-Arg-Ala-C	-35.3
Peptide ligand 2	N-Cys-Ile-Ala-Lys-Arg-Ile-Ile-Ala-Arg-Arg-C	-36.2
Peptide ligand 3	N-Cys-Met-Ile-Lys-Lys-Arg-Ala-Ala-Arg-Ile-C	-38.5
Peptide ligand 4	N-Cys-Arg-Arg-Ile-Ile-Arg-Ala-Ala-Arg-Met-C	-39.7
Peptide ligand 5	N-Cys-Ser-Arg-Arg-Ser-Lys-Met-Ser-Lys-Lys-C	-42.6
Peptide ligand 6	N-Cys-Met-Ser-Ser-Lys-Arg-Arg-Ile-Ile-Lys-C	-42.4
Peptide ligand 7	N-Cys-Met-Ser-Lys-Ser-Lys-Met-Lys-Lys-Met-C	-45.6
Peptide ligand 8	N-Cys-Cys-Lys-Lys-Arg-Met-Arg-Ile-Lys-Ile-C	-46.4
Peptide ligand 9	N-Cys-Cys-Lys-Arg-Lys-Arg-Ile-Lys-Cys-Cys-C	-47.8
Peptide ligand 10	N-Cys-Lys-Lys-Arg-Met-Met-Lys-Ser-Met-Cys-C	-48.6

### 2.10. Assessment of Sap activity

To evaluate Sap activity, spectrophotometric assessment was done. First, 0.1 mL of culture supernatant and 0.4 mL of 0.1 M sodium citrate buffer (pH 3.2) containing BSA 1% w/v were added, and incubated for 15 min at 37 °C. In the control tube, 0.1 mL of 50 µg/mL pepstatin A was used instead of culture supernatant. Then, 0.5 mL of 5% TCA was added to stop reaction. The mixture was centrifuged at 10,000 rpm for 10 min, and the OD of each tube was read at 280 nm against distilled water. Enzyme activity was expressed as the amount (µM) of tyrosine equivalents released per min per ml of culture supernatant [23].

### 2.11. Statistical analysis

All tests were carried out three times, and the results were shown as the mean ± standard deviation (SD). Student's *t*-test was used, to detect significant difference by SPSS software (version 16.0 for Windows; SPSS Inc., USA), and *P* value <0.05 was regarded as statistically significant.

## 3. Results

### 3.1. Selection of peptide ligands based on software data

As described, 10 peptide ligands with the lowest intermolecular energy were finally selected. Table 1 shows the sequence and intermolecular energy of all selected peptide ligands. The best result was observed for peptide ligand 10, containing N-Cys-Lys-Lys-Arg-Met-Met-Lys-Ser-Met-Cys-C. As seen, the intermolecular energy between peptide ligand 10 and Sap2 enzyme was -48.6 kcal/mol.

### 3.2. Characterization of triangular gold nanoparticles

UV-vis spectrum, DLS graph, and TEM image are shown in Fig. 1a–c, respectively. Fig. 1a shows that triangular gold nanoparticles have two sharp peaks at 540 nm and 750 nm. Based on Fig. 1b, the size distribution of triangular gold nanoparticles was near 1–120 nm, and the average of particles was approximately 30 nm. Also, Fig. 1c confirmed triangular shape of gold nanoparticles.

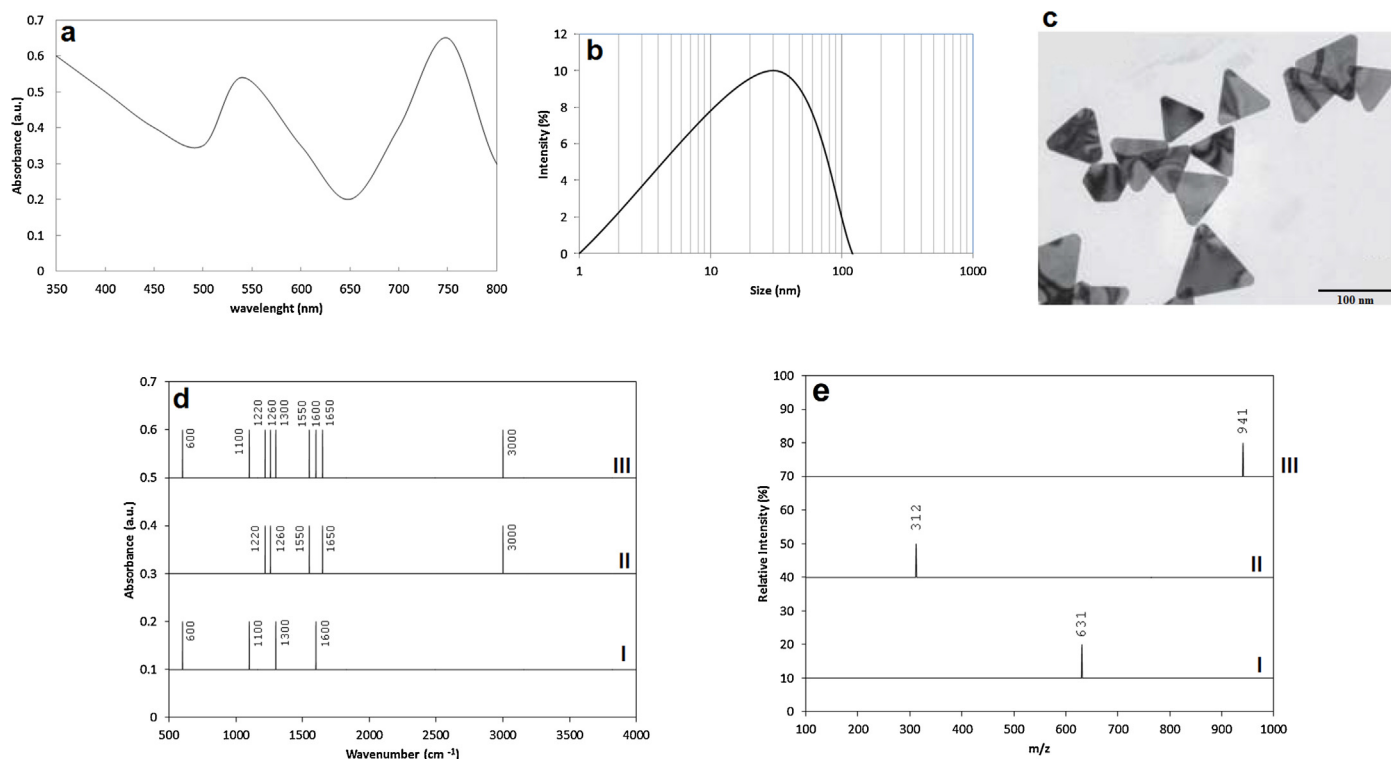


**Fig. 1.** Characterization of triangular gold nanoparticles. UV-vis spectrum (a), DLS graph (b), TEM image of triangular gold nanoparticles (c), FTIR spectrum (d) of triangular gold nanoparticles (I), peptide ligand 10 (II), and conjugated triangular gold nanoparticle 10 (III). The MS peak (e) of triangular gold nanoparticles (I), peptide ligand 10 (II), and conjugated triangular gold nanoparticle 10 (III).

### 3.3. Conjugation of selected peptide and triangular gold nanoparticles

As mentioned, to confirm conjugation of peptide ligands and triangular gold nanoparticles, FTIR and MS were used. Fig. 1d shows the spectrum of triangular gold nanoparticles (I), peptide ligand 10 (II), and conjugated triangular gold nanoparticles (III). As demonstrated, both peptide ligand 10 and its conjugate have sharp bands at 1220, 1260, 1550, and 1650  $\text{cm}^{-1}$  which confirmed conjugation. Moreover, the MS peaks of triangular gold nanoparticles (I), peptide ligand 10 (II), and conjugated triangular gold nanoparticles (III) are 631, 312, and 941  $m/z$ , respectively (Fig. 1e). Since all peptide ligands and their conjugates had the same spectrum and peak, we did not show others, and they have been omitted.

### 3.4. The result of micro-dilution and agar disk diffusion

The MIC50, MIC90, and inhibition zone of 10 conjugated triangular gold nanoparticles, 10 peptide ligands, and triangular gold nanoparticle alone against thirty isolates of *C. albicans* are shown in Table 2. As seen, the MIC50 of each conjugated triangular gold nanoparticle was less than the MIC50 of peptide ligand with same number ( $P < 0.05$ ). Exactly, this pattern was seen for the MIC90 of each conjugate and its peptide ligand ( $P < 0.05$ ). Moreover, it was shown that no peptide ligands had inhibition zone, but all conjugated triangular gold nanoparticles had inhibition zone between 14 and 20 mm. Significant difference was seen between inhibition zone of conjugated triangular gold nanoparticle 10 and triangular gold nanoparticle alone ( $P < 0.05$ ). The best antifungal activity was shown for the conjugated triangular gold nanoparticle 10. The MIC50, MIC90, and inhibition zone of conjugated triangular gold nanoparticle 10 was  $20 \pm 1$  ( $\mu\text{g}/\text{mL}$ ),  $45 \pm 2$  ( $\mu\text{g}/\text{mL}$ ), and  $15 \pm 1$  mm, respectively.

### 3.5. The uptake assay results

The uptake of three concentrations of each conjugated triangular gold nanoparticle and triangular gold nanoparticle

alone after 24 and 48 h is shown in Fig. 2a and b, respectively. As seen, *Candida* cells which are treated for 24 and 48 h with conjugated triangular gold nanoparticles 1, 2, 3, 4, 5, 6, 7, and triangular gold nanoparticle alone had approximately same uptake. In the case of conjugated triangular gold nanoparticles 8, 9, and 10, an increase of uptake was seen. There were significant differences between the uptake of conjugated triangular gold nanoparticles 8, 9, 10 and the uptake of conjugated triangular gold nanoparticles 1, 2, 3, 4, 5, 6, 7. As important finding, the more concentration and incubation time, the more uptake, i.e. the uptake was dose and time dependent, especially in case of conjugated triangular gold nanoparticles 8, 9, 10. The highest uptake, near  $14 \mu\text{M}$ , was observed for the cells incubated with conjugated triangular gold nanoparticle 10 at a concentration of  $64 \mu\text{g}/\text{mL}$  for 48 h.

### 3.6. The Sap activity results

Fig. 2c and d shows the Sap activity when *Candida* cells are incubated with three concentrations of conjugated triangular gold nanoparticles, peptide ligands, and triangular gold nanoparticle alone for 48 and 24 h, respectively. As the first finding, the same pattern of Sap activity was seen for each conjugated triangular gold nanoparticle and its peptide ligand. As second finding, the higher concentration and incubation time led to more decrease of Sap activity. As third finding, the lowest Sap activity ( $0.5 \mu\text{M}$ ) was for conjugated triangular gold nanoparticles 9, 10 and peptide ligands 9, 10. The Sap activity was for concentration of  $64 \mu\text{g}/\text{mL}$  and incubation time of 48 h.

## 4. Discussion

Although Sap enzyme is a key virulence factor of *C. albicans*, it can be inactivated by different biomolecules such as antibody [13], pepstatin [14], peptidomimetic inhibitors [15], and renin inhibitors [16]. Here, we wanted to find and design synthetic small peptides for inhibition of *C. albicans* Sap2 enzyme.

**Table 2**  
The MIC50, MIC90, and inhibition zone of 10 conjugated triangular gold nanoparticles, 10 peptide ligands, and triangular gold nanoparticles alone against thirty isolates of *Candida albicans*.

	MIC50 ( $\mu\text{g}/\text{mL}$ )	MIC90 ( $\mu\text{g}/\text{mL}$ )	Inhibition zone (mm)
Conjugated triangular gold nanoparticle 1	$24 \pm 1^{*,\#}$	$64 \pm 3^{##}$	$14 \pm 1^{***}$
Conjugated triangular gold nanoparticle 2	$25 \pm 1^{*,\#}$	$64 \pm 2^{##}$	$15 \pm 1^{***}$
Conjugated triangular gold nanoparticle 3	$20 \pm 0.5^*$	$61 \pm 2^{**,\#,\#}$	$14 \pm 1^{***}$
Conjugated triangular gold nanoparticle 4	$19 \pm 0.5^*$	$62 \pm 2^{**,\#,\#}$	$15 \pm 0.5^{***}$
Conjugated triangular gold nanoparticle 5	$19 \pm 1^*$	$56 \pm 1^{**,\#,\#}$	$15 \pm 1^{***}$
Conjugated triangular gold nanoparticle 6	$18 \pm 1^*$	$49 \pm 2^{**,\#,\#}$	$16 \pm 1^{***}$
Conjugated triangular gold nanoparticle 7	$16 \pm 0.5^{*,\#}$	$46 \pm 2^{**}$	$18 \pm 0.5^{***,\#,\#,\#}$
Conjugated triangular gold nanoparticle 8	$15 \pm 0.2^{*,\#}$	$45 \pm 1^{**}$	$18 \pm 1^{***,\#,\#,\#}$
Conjugated triangular gold nanoparticle 9	$12 \pm 0.1^{*,\#}$	$40 \pm 1^{**}$	$19 \pm 1^{***,\#,\#,\#}$
Conjugated triangular gold nanoparticle 10	$10 \pm 1^{*,\#}$	$39 \pm 1^{**}$	$20 \pm 1^{***,\#,\#,\#}$
Peptide ligand 1	$>64^{\#}$	$>64^{\#,\#}$	NO <sup>a</sup>
Peptide ligand 2	$>64^{\#}$	$>64^{\#,\#}$	NO
Peptide ligand 3	$>64^{\#}$	$>64^{\#,\#}$	NO
Peptide ligand 4	$>64^{\#}$	$>64^{\#,\#}$	NO
Peptide ligand 5	$>64^{\#}$	$>64^{\#,\#}$	NO
Peptide ligand 6	$>64^{\#}$	$>64^{\#,\#}$	NO
Peptide ligand 7	$>64^{\#}$	$>64^{\#,\#}$	NO
Peptide ligand 8	$>64^{\#}$	$>64^{\#,\#}$	NO
Peptide ligand 9	$>64^{\#}$	$>64^{\#,\#}$	NO
Peptide ligand 10	$>64^{\#}$	$>64^{\#,\#}$	NO
Triangular gold nanoparticle	$20 \pm 1$	$45 \pm 2$	$15 \pm 1$

<sup>a</sup> Not observed.

\*  $P < 0.05$  compared with MIC50 of peptide ligand with same number.

\*\*  $P < 0.05$  compared with MIC90 of peptide ligand with same number.

\*\*\*  $P < 0.05$  compared with inhibition zone of peptide ligand with same number.

#  $P < 0.05$  compared with MIC50 of triangular gold nanoparticle.

##  $P < 0.05$  compared with MIC90 of triangular gold nanoparticle alone.

###  $P < 0.05$  compared with inhibition zone of triangular gold nanoparticle.



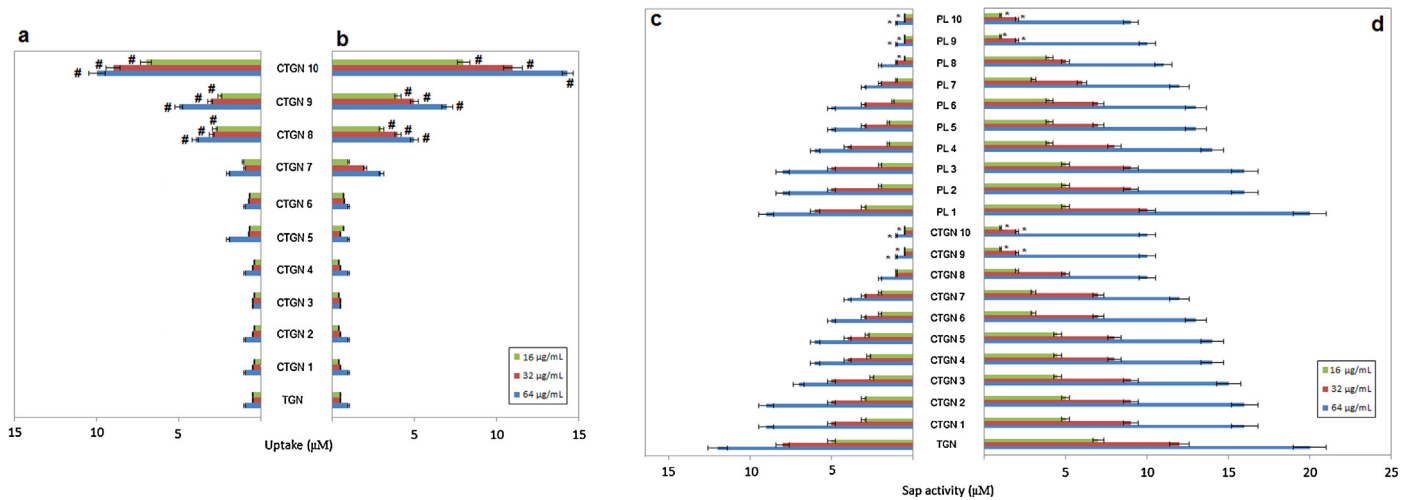


**Fig. 2.** The uptake of conjugated triangular gold nanoparticles (CTGNs) and triangular gold nanoparticles (TGNs) after 24 h (a) and 48 h (b). The Sap activity when *Candida* isolates incubated with conjugated triangular gold nanoparticles, peptide ligands (PLs), and triangular gold nanoparticles alone after 48 h (c) and 24 h (d). # $P < 0.05$  compared with the uptake of conjugated triangular gold nanoparticles 1, 2, 3, 4, 5, 6, 7, and triangular gold nanoparticles. \* $P < 0.05$  compared with the Sap activity of conjugated triangular gold nanoparticles 1, 2, 3, 4, 5, 6, 7 and peptide ligands 1, 2, 3, 4, 5, 6, 7.

In the first step, a ligand library, containing 300 different peptides, was performed. The library was based on X-ray crystallography and pdb file of Sap enzyme. Generally, active site of Sap enzyme has several aspartyl residues which gives negative charge to it. Based on Fig. 3, the size of Sap active site was near 2 nm [17], and it seemed that the peptides with 10 amino acids with positive charge were suitable to interact with Sap active site. We listed 300 different peptides, and then the interaction of each peptide with Sap2 enzyme was calculated by Ascalaph Designer, as molecular dynamic software. It must be mentioned that the N-end of all peptides had Cys amino acid, because the amino acid can be conjugated with gold nanoparticles by thiol–gold interaction. Finally, intermolecular energy was separately measured for each

peptide and Sap2, and 10 peptide ligands with the lowest intermolecular energy were chosen (Table 1).

In the next step, triangular gold nanoparticles were synthesized and characterized. In our previous study, we worked on the antifungal properties of different shapes of gold and silver nanoparticles [20]. We evaluated nanocubes, nanospheres, and nanowires, and it was found that silver and gold nanocubes had the highest antifungal activity against *C. albicans*, *Candida glabrata* and *C. tropicalis*. For the first time, Smitha et al. [24] showed high antimicrobial activity of triangular gold nanoparticles against *Escherichia coli*, *Staphylococcus aureus*, *Aspergillus niger*, and *Fusarium oxysporum*. Here, after synthesis of triangular gold nanoparticles according to Miranda article [19], selected peptide

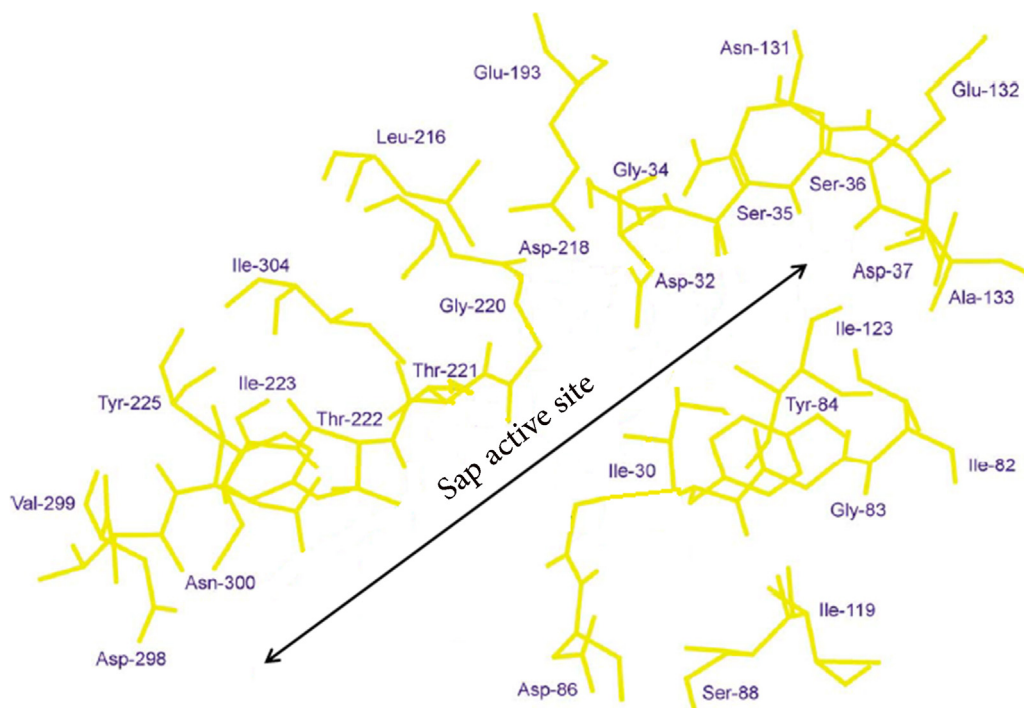


**Fig. 3.** The schematic representation of Sap2 active site.

ligands were separately conjugated with synthesized gold nanoparticles. As mentioned earlier, triangular gold nanoparticles and peptide ligands were attached by thiol–gold interaction, and confirmed by FTIR.

After synthesis and characterization, antifungal activity of triangular gold nanoparticles, peptide ligands, and conjugated triangular gold nanoparticles against thirty clinical isolates of *C. albicans* obtained from patients suffering from vaginal candidiasis was evaluated by micro-dilution and agar disk diffusion method. As demonstrated, the MIC<sub>50</sub> of conjugated triangular gold nanoparticles 4, 5, 6, 7, 8, 9, and 10 was less than MIC<sub>50</sub> of triangular gold nanoparticle alone, and the MIC<sub>50</sub> of other conjugated triangular gold nanoparticles and all peptide ligands were more than the MIC<sub>50</sub> of triangular gold nanoparticle alone. Moreover, the MIC<sub>90</sub> of conjugated triangular gold nanoparticles 9 and 10 was less than MIC<sub>90</sub> of triangular gold nanoparticle alone, and other conjugated triangular gold nanoparticles and all peptide ligands had bigger MIC<sub>90</sub> than triangular gold nanoparticle alone. On the other hand, the MIC<sub>50</sub> and MIC<sub>90</sub> of each conjugated triangular gold nanoparticle was less than the MIC<sub>50</sub> and MIC<sub>90</sub> of peptide ligand with same number ( $P < 0.05$ ). Importantly, no inhibition zone was seen for peptide ligands, but all conjugated triangular gold nanoparticles had remarkably inhibition zone, between 14 and 20 mm. It was shown that the inhibition zone of conjugated triangular gold nanoparticles 6, 7, 8, 9, and 10 was higher than the inhibition zone of triangular gold nanoparticle alone. Among all conjugated triangular gold nanoparticles, conjugated triangular gold nanoparticle 10 had the highest antifungal activity, and its MIC<sub>50</sub>, MIC<sub>90</sub>, and inhibition zone was  $20 \pm 1$  ( $\mu\text{g/mL}$ ),  $45 \pm 2$  ( $\mu\text{g/mL}$ ), and  $15 \pm 1$  mm, respectively. Overall, this study showed antifungal activity of triangular gold nanoparticle, which has been mentioned in the Smitha et al. work. As a new result, we demonstrated that conjugated triangular gold nanoparticles 8, 9, and 10 had higher antifungal activity than other conjugated triangular gold nanoparticles and triangular gold nanoparticle alone. We propose that the higher uptake of conjugated triangular gold nanoparticles 8, 9, and 10 may be the reason of their higher antifungal activity. As seen, *Candida* cells which incubated with conjugated triangular gold nanoparticles 1, 2, 3, 4, 5, 6, and 7 had approximately same uptake, but conjugated triangular gold nanoparticles 8, 9, and 10 had significantly higher uptake. The reason for high uptake of conjugated triangular gold nanoparticles 8, 9, and 10 is questionable, and must be studied in the future studies. It was hypothesized that conjugated triangular gold nanoparticles 8, 9, and 10 could stimulate receptor-mediated endocytosis.

This study showed that conjugated triangular gold nanoparticles 9, 10 and peptide ligands 9, 10 had the highest power to inhibit the Sap2 enzyme. Also, we found that the higher concentration and incubation time led to less Sap activity. Based on Fig. 2c and d, the lowest Sap activity, near  $0.5 \mu\text{M}$ , was for conjugated triangular gold nanoparticles 9, 10 and peptide ligands 9, 10 at concentration of  $64 \mu\text{g/mL}$  and incubation time of 48 h. The reason of the highest inhibition activity of conjugated triangular gold nanoparticles 9, 10 and peptide ligands 9, 10 may be due to their highest interaction between them and Sap enzyme. The result is in consistent with simulation data. As shown in Table 1, the sequence of peptide ligands 9 and 10 was N-Cys-Cys-Lys-Arg-Lys-Arg-Ile-Lys-Cys-Cys-C and N-Cys-Lys-Lys-Arg-Met-Met-Lys-Ser-Met-Cys-C, respectively.

The design of Sap inhibitors by computer-based method has been previously done by Cele Abad-Zapatero at Abbott Laboratories [25]. They found that Sap2 activity could be inhibited by some renin inhibitors such as A-70450 and A-79912. Also, Cadicamo et al. designed and synthesized three libraries of inhibitors, based on the structure of pepstatin A with some changes at the P<sub>3</sub>, P<sub>2</sub>, and P<sub>2'</sub> position. They showed that these inhibitors had high

inhibitory potencies against *C. albicans* Sap1, Sap3, Sap5 and Sap6 [26]. Importantly, these inhibitors may have several problems when used in vivo including the lack of protection, lack of inhibitor potency, and the lack of specificity. It must be mentioned all of restrictions may be existed for our work, and must be checked in the future study. In conclusion, we presented some peptide ligands which inhibited *C. albicans* Sap2 enzyme. Moreover, triangular gold nanoparticle conjugated with the peptide ligands had high antifungal property, and could inhibit Sap2.

## Conflicts of interest

No conflict of interest was addressed.

## Acknowledgments

This article financially supported by Farzaneh Haji Esmaeil Hajjar (Grant number 2-2013) and Department of Medical Nanotechnology, Pajoohesh Lab, Yazd, Iran (Grant number 1-2013). The authors thank the laboratory staff of the Yazd Pajoohesh medical lab. Jesus M. de la Fuente thanks MAT2011-26851-C02-01, Fondo Social Europeo, ERC-Starting Grant 239931-NANOPUZZLE, CDTI-INMUNOSWING, Shanghai 100 People Plan and ARAID for financial support.

## References

- Reichard U, Cole GT, Ruchel R, Monod M. Molecular cloning and targeted deletion of PEP2 which encodes a novel aspartic proteinase from *Aspergillus fumigatus*. *Int J Med Microbiol* 2000;290:85–96.
- Cafarchia C, Figueredo LA, Coccioli C, Camarda A, Otranto D. Enzymatic activity of *Microsporium canis* and *Trichophyton mentagrophytes* from breeding rabbits with and without skin lesions. *Mycoses* 2012;55:45–9.
- Aoki S, Ito-Kuwa S, Nakamura K, Kato J, Ninomiya K, Vidotto V. Extracellular proteolytic activity of *Cryptococcus neoformans*. *Mycopathologia* 1994;128:143–50.
- De Bernardis F, Sullivan PA, Cassone A. Aspartyl proteinases of *Candida albicans* and their role in pathogenicity. *Med Mycol* 2001;39:303–13.
- Boriollo MF, Bassi RC, dos Santos Nascimento CM, Feliciano LM, Francisco SB, Barros LM, et al. Distribution and hydrolytic enzyme characteristics of *Candida albicans* strains isolated from diabetic patients and their non-diabetic consorts. *Oral Microbiol Immunol* 2009;24:437–50.
- Rajendran R, Robertson DP, Hodge PJ, Lappin DF, Ramage G. Hydrolytic enzyme production is associated with *Candida albicans* biofilm formation from patients with type 1 diabetes. *Mycopathologia* 2010;170:229–35.
- Kalkanci A, Bozdayi G, Biri A, Kustimur S. Distribution of secreted aspartyl proteinases using a polymerase chain reaction assay with SAP specific primers in *Candida albicans* isolates. *Folia Microbiol (Praha)* 2005;50:409–13.
- Schaller M, Januschke E, Schackert C, Woerle B, Korting HC. Different isoforms of secreted aspartyl proteinases (Sap) are expressed by *Candida albicans* during oral and cutaneous candidosis in vivo. *J Med Microbiol* 2001;50:743–7.
- Magee BB, Hube B, Wright RJ, Sullivan PJ, Magee PT. The genes encoding the secreted aspartyl proteinases of *Candida albicans* constitute a family with at least three members. *Infect Immun* 1993;61:3240–3.
- Gilfillan GD, Sullivan DJ, Haynes K, Parkinson T, Coleman DC, Gow NA. *Candida dubliniensis*: phylogeny and putative virulence factors. *Microbiology* 1998;144(Pt 4):829–38.
- Zaug C, Borg-Von Zepelin M, Reichard U, Sanglard D, Monod M. Secreted aspartic proteinase family of *Candida tropicalis*. *Infect Immun* 2001;69:405–12.
- de Viragh PA, Sanglard D, Togni G, Falchetto R, Monod M. Cloning and sequencing of two *Candida parapsilosis* genes encoding acid proteases. *J Gen Microbiol* 1993;139:335–42.
- Rodrigues JA, Hofling JF, Azevedo RA, Gabriel DL, Tamashiro WM. Production of monoclonal antibodies for detection of a secreted aspartyl proteinase from *Candida* spp. in biologic specimens. *Hybridoma (Larchmt)* 2007;26:201–10.
- Leto G, Pizzolanti G, Tumminello FM, Gebbia N. Effects of E-64 (cysteine-proteinase inhibitor) and pepstatin (aspartyl-proteinase inhibitor) on metastasis formation in mice with mammary and ovarian tumors. *In Vivo* 1994;8:231–6.
- Pichova I, Pavlickova L, Dostal J, Dolejsi E, Hruskova-Heidingsfeldova O, Weber J, et al. Secreted aspartic proteases of *Candida albicans*, *Candida tropicalis*, *Candida parapsilosis* and *Candida lusitanae*. Inhibition with peptidomimetic inhibitors. *Eur J Biochem* 2001;268:2669–77.
- Cutfield SM, Dodson EJ, Anderson BF, Moody PC, Marshall CJ, Sullivan PA, et al. The crystal structure of a major secreted aspartic proteinase from *Candida albicans* in complexes with two inhibitors. *Structure* 1995;3:1261–71.

- [17] Pranav Kumar SK, Kulkarni VM. Insights into the selective inhibition of *Candida albicans* secreted aspartyl protease: a docking analysis study. *Bioorg Med Chem* 2002;10:1153–70.
- [18] Yadav VK, Mandal RS, Puniya BL, Singh S, Yadav S. Studies on the interactions of SAP-1 (an N-terminal truncated form of cystatin S) with its binding partners by CD-spectroscopic and molecular docking methods. *J Biomol Struct Dyn* 2013.
- [19] Miranda A, Malheiro E, Skiba E, Quaresma P, Carvalho PA, Eaton P, et al. One-pot synthesis of triangular gold nanoplates allowing broad and fine tuning of edge length. *Nanoscale* 2010;2:2209–16.
- [20] Jebali A, Hajjar FH, Pourdanesh F, Hekmatimoghaddam S, Kazemi B, Masoudi A, et al. Silver and gold nanostructures: antifungal property of different shapes of these nanostructures on *Candida* species. *Med Mycol* 2013.
- [21] Jebali A, Kazemi B. Nano-based antileishmanial agents: a toxicological study on nanoparticles for future treatment of cutaneous leishmaniasis. *Toxicol In Vitro* 2013;27:1896–904.
- [22] Jebali A, Kazemi B. Triglyceride-coated nanoparticles: skin toxicity and effect of UV/IR irradiation on them. *Toxicol In Vitro* 2013;27:1847–54.
- [23] Rehani S, Rao NN, Rao A, Carmelio S, Ramakrishnaiah SH, Prakash PY. Spectrophotometric analysis of the expression of secreted aspartyl proteinases from *Candida* in leukoplakia and oral squamous cell carcinoma. *J Oral Sci* 2011;53:421–5.
- [24] Smitha SL, Gopchandran KG. Surface enhanced Raman scattering, antibacterial and antifungal active triangular gold nanoparticles. *Spectrochim Acta A Mol Biomol Spectrosc* 2013;102:114–9.
- [25] Goldman RC, Frost DJ, Capobianco JO, Kadam S, Rasmussen RR, Abad-Zapatero C. Antifungal drug targets: *Candida* secreted aspartyl protease and fungal wall beta-glucan synthesis. *Infect Agents Dis* 1995;4:228–47.
- [26] Cadicamo CD, Mortier J, Wolber G, Hell M, Heinrich IE, Michel D, et al. Design, synthesis, inhibition studies, and molecular modeling of pepstatin analogues addressing different secreted aspartic proteinases of *Candida albicans*. *Biochem Pharmacol* 2013;85:881–7.